# Progress in metal-insulator-metal waveguide lasers at near-infrared wavelengths

# Progress in Metal-insulator-metal Waveguide Lasers at Near-infrared Wavelengths

**Milan J. H. Marell and Martin T. Hill**
COBRA Research Institute, Technische Universiteit Eindhoven
Postbus 513, 5600 MB Eindhoven, The Netherlands

**Abstract**— Strong light confinement can be achieved in metallic cavities which can confine light to volumes with dimensions considerably smaller than the wavelength of light. It was commonly believed, however, that the high losses in metals are prohibitive for laser operation in metallic nano-cavities. Recently we have reported lasing in a metallic nano-cavity filled with an electrically pumped semiconductor. Importantly, the manufacturing approach employed for these devices permits even greater miniaturization of semiconductor lasers. Furthermore, the approach allows for complex device shapes and the guiding of light between devices. Of particular interest are the metal-insulator-metal (MIM) waveguides. These MIM waveguides can propagate a transverse magnetic (TM0) mode which permits true deep sub-wavelength guiding of light in two dimensions. The manufacturing process is adapted to produce a variant of MIM waveguides. The presentation will look at the modeling, fabrication and operation of these devices. An overview will also be given of latest results from devices.

Previously reported devices observed light that leaked out of the metallic nano cavity through the device base. This is not optimal as the lasing light travels transversally between the metal sidewalls of the pillar structure. Ideally, the transverse propagating mode needs to be coupled directly out to either a conventional dielectric waveguide or free space. We will discuss our progress in making metallic cavity nano lasers with coupling of the transverse propagating mode directly to free space, and present results from our latest attempts.

## 1. INTRODUCTION

So far all metallic waveguide lasers have been characterized by observing light leaking through the substrate of the chip [1]. This poses difficulties with respect to their integrability in photonic circuits. Ideally the propagating mode of such a device is coupled out directly to free space or a waveguide. There are various ways in which this can be done.

In order to sustain laser operation, only a fraction of the light can be extracted from the cavity. This can be realized by incorporating a Bragg reflector at the junction with the laser. However, recent experiments show that also a cleaved facet provides sufficient reflectivity.

## 2. FABRICATION

The side-emitting structures are fabricated on InP/InGaAsP/InP wafers, in which 8 InGaAs quantum wells are incorporated. The quantum wells are 4.1 nm thick and the total thickness of the film layer is 510 nm. The high index contrast between the InGaAs core and InP cladding layers provides vertical confinement.

The rectangular cross-section of the structures is defined by means of electron beam lithography and lift-off the width of the structures varies from 100 nm to 250 nm. After plasma etching with a $CH_4/H_2$ chemistry in an ICP system, the structures are covered with a 20 nm thick $Si_3N_4$ layer, which serves as electrical insulation. Finally the devices are encapsulated in metal and additional metal layers are deposited to form the top contact. A more detailed description of the manufacturing process is given in [1].

After fabrication the structures are cleaved in half, forming two devices with one open facet and one covered with metal, Figure 1.

## 3. CHARACTERIZATION

The first side-emitting metallic lasers have been characterized in a cryostat at a temperature of 80 K. At low temperatures semiconductor gain is higher, non-radiative recombination lower, and the metal can have lower optical losses. Hence, at lower temperatures the structures are more likely to lase. The results of CW current injection measurements are shown in Figures 1 and 2.

From Figure 3.1, it can be seen that the threshold current of the metallic lasers is less than 0.5 mA and the free spectral range is 4.47 nm. At $I = 1.5$ mA the side mode suppression ratio is

22.63 dB and the laser peak is approximately 26 dB above the spontaneous emission level. This is shown in Figures 2 and 3. The length of the waveguide was measured to be approximately 62 μm.

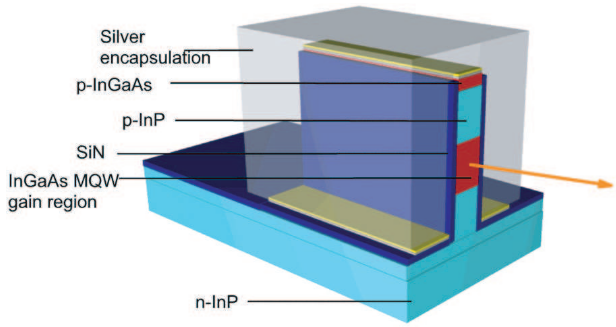


Figure 1: Schematic overview of a device after processing.

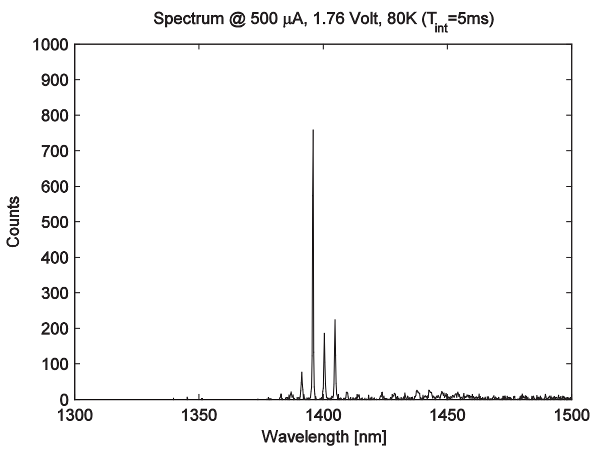


Figure 2: Power spectrum of the device just above threshold at an injection current of $I_{dev} = 0.5$ mA.

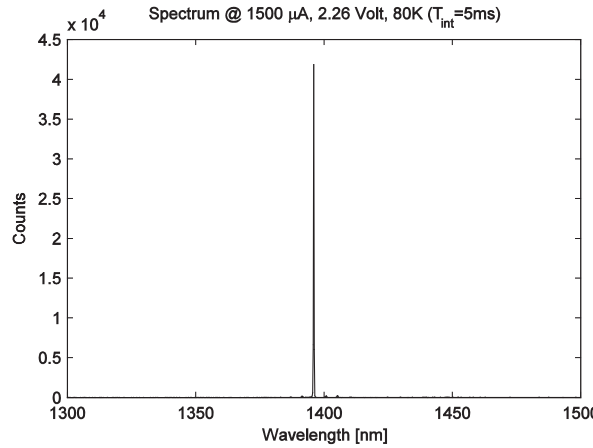


Figure 3: Power spectrum of the device well above the threshold ($I_{dev} = 1.5$ mA). One laser peak remains at a wavelength of 1396 nm.

Figure 4 shows the L-I curve of the measured device. The device does not exhibit a strong super linear L-I characteristic. This may be due to either strong coupling of spontaneous emission to the resonant modes, or possibly heating in the devices. The exact cause is under investigation.

CW Measurements have been performed for temperatures up to 200 K, the limiting factor being the current source. It is expected that lasing at room temperature is possible for pulsed current injection. These measurements, however, still need to be carried out.

## 4. FUTURE WORK

From the Figures 2 and 3, it can be seen that the lasing wavelength differs from the desired telecom wavelength range around 1550 nm. This can be explained by the gain material not being optimized for this purpose. In future devices a wavelength selective mirror (DBR) will be incorporated and better designed gain regions employed to achieve lasing at the desired wavelength.

FDTD Software is used to analyze the laser structures without gain. From these simulations facet reflectivities, propagation loss and optimal device dimensions can be estimated. In this section we will report briefly on the simulations we have done to determine the dimensions of the DBR reflector which we plan to use in future devices.

2D FDTD simulations have been performed. In the simulations the different materials are represented by their dielectric constant. The dielectric constant of silver is accounted for via a Lorentzian oscillator (Equation (1)), of which the parameters are chosen to match the complex

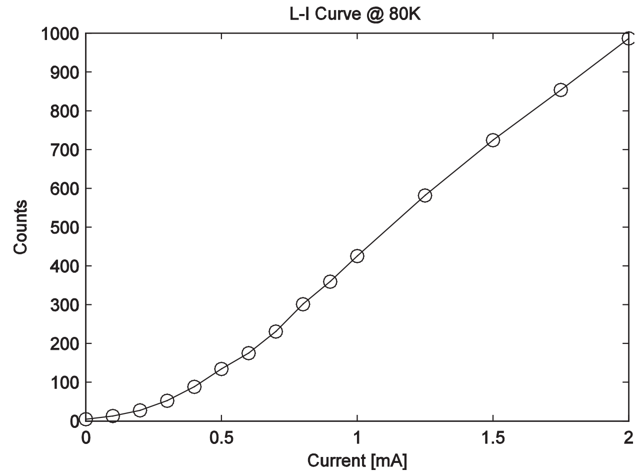


Figure 4: L-I curve of a metallic laser.

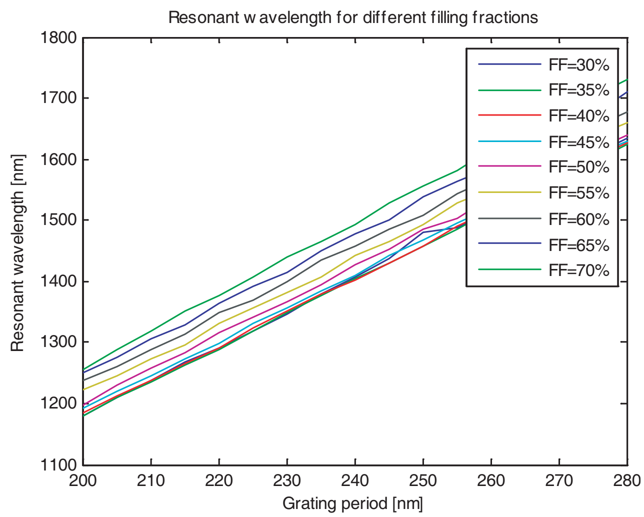


Figure 5: Results of 2D FDTD simulations of a unit cell of a metallic grating. The figure shows the resonant wavelength as a function of grating period and filling fraction (FF) defined as the fraction of outer width waveguide in a grating period.

refractive index data in the Johnson & Christy paper (2) in the wavelength range of 1 μm to 2 μm.

$$\varepsilon(\omega) = \varepsilon_\infty + \sum_n \frac{\Delta\varepsilon \cdot \omega_n^2}{\omega_n^2 - \omega^2 - i\gamma\omega} \tag{1}$$

The grating dimensions were determined by performing unit cell simulations of the structure. In these unit cell simulations inner width of the waveguide was 100 nm and the outer width of the waveguide 200 nm. The thickness of the $Si_3N_4$ layer was 20 nm throughout the simulations. Exclusion of the 3rd dimension in the simulations leads to a minor deviation in the resonant wavelength. More accurate 3D analysis can be performed as soon as feedback from fabrication and characterization is available.

## 5. CONCLUSIONS

We have shown that, despite high propagation loss in metallic waveguides, it is possible to fabricate side-emitting metallic lasers. The tested device has a side mode suppression ratio of ±23 dB and a free spectral range of 4.47 nm.

With around 0.3 mA, the threshold current of these lasers is considerably lower compared to conventional semiconductor lasers in this wavelength range. Currently the side-emitting metallic lasers operate at cryogenic temperatures $< 200$ K (CW), but room-temperature operation is expected for pulsed current injection.

The emission wavelength of 1396 nm is due to the material not being optimal for this purpose. Lasing at telecom wavelengths (i.e., 1550 nm) may be achieved by tuning the dimensions of the device and by incorporation of a wavelength dependent feedback mechanism, such as a distributed Bragg reflector.

## REFERENCES

1. Hill, M. T., Y. S. Oei, B. Smalbrugge, et al., "Lasing in metallic-coated nanocavities," *Nature Photonics*, Vol. 1, No. 10, 589–594, October 2007.
2. Johnson, P. B. and R. W. Christy, "Optical constants of the noble metals," *Phys. Rev. B*, Vol. 6, No. 12, 4370–4379, 1972.